A novel concept for finding proper orthogonal wavelets effectively to solve a large object scattering problem

Chih-Ming Chen, Jenn-Hwan Tarng, and Jiunn-Ming Huang

Department of Communication Engineering and Microelectronics and Information Systems Research Center, National Chiao Tung University, Hsin-Chu, Taiwan

Received 4 April 2001; revised 13 March 2002; accepted 8 July 2002; published 18 April 2003.

[1] A novel concept of "visible energy" is proposed, and its magnitude is shown to be valuable information for determining whether the chosen orthogonal wavelet is proper in solving a large object scattering problem. With the properly chosen wavelets for the targeting problem the (transformed) wavelet-domain impedance matrix can be sparsified effectively for solving electromagnetic integral problems. Visible energy is defined as the energy of all dilations of a single mother wavelet for an arbitrary translation in the spectral domain over the entire "visible region." It is found that for large matrix sizes, using wavelets with smaller visible energy will lead to a greater sparsification of the matrix. Numerical examples considering various scatterers with different shapes such as a circular cylinder, an L-shaped scatterer, and a duct show the validity of our findings. *INDEX TERMS:* 0619 Electromagnetics: Electromagnetic theory; 0644 Electromagnetics: Numerical methods; 0669 Electromagnetics: Scattering and diffraction; 0689Electromagnetics: Wave propagation (4275); *KEYWORDS:* orthogonal wavelets, visible energy, sparsification

Citation: Chen, C.-M., J.-H. Tarng, and J.-M. Huang, A novel concept for finding proper orthogonal wavelets effectively to solve a large object scattering problem, *Radio Sci., 38*(2), 1029, doi:10.1029/2001RS002475, 2003.

1. Introduction

[2] Radiated emission of electromagnetic energy is one of the major aspects of the electromagnetic compatibility (EMC) problem. To study this problem, it is necessary to understand the electromagnetic field distribution in the surrounding environment, which may consist of various dielectric media and conducting objects. Generally, EMC problems are relatively complicated and usually cannot be solved analytically, so that numerical analysis techniques must be used. Numerical analysis techniques include method of moment (MoM) [*Harrington*, 1968; *Miller and Landt*, 1980; *Bernardi et al*., 1996], the finite difference time domain method [*Tirkas et al.*, 1993; *Taflove and Umashankar*, 1989], the transmission line matrix method [*Christopoulos and Herring*, 1993; *D'amore and Sarto*, 1996], the finite element method [*Dixon et al.*, 1993; *Sacks and Lee*, 1995], and the finite volume time domain method [*Holland et al.*, 1991]. These methods have been successfully applied in solving electromagnetic scattering problems in EMC-related fields such as antennae, microwave, and millimeter wave circuits and radar cross sections.

[3] MoM is a well-established numerical method and is probably the most widely used technique for solving integral equations in electromagnetics. In conventional MoM the boundary of integration is approximated by discretizing it into many segments, and then the unknown function is expanded in terms of known basis functions with unknown coefficients. However, classical subsectional bases, when applied directly to the integral equations, generally produce a dense impedance matrix. The dense matrix often becomes computationally unmanageable owing to the large memory requirement and CPU time required to invert the dense matrix. Recently, the use of wavelets and wavelet-like basis functions for the efficient solution of electromagnetic integral equations has received considerable attention. The wavelet bases have been used to overcome the major drawback mentioned above and to sparsify the matrix, primarily because of local supports and vanishing moment properties of the wavelet bases.

[4] *Beylkin et al.* [1991] first applied wavelets to the solution of integral equations having essentially smooth, nonoscillatory kernels, such as those encountered in electrostatics. For electrodynamic problems, however, the Green's function (kernel) is oscillatory in the spectral frequency domain which leads to a dense impedance matrix. Hence many other researchers applied different wavelet transform methods to effectively sparsify the impedance matrix in MoM. *Kim et al.* [1996] used spectral domain wavelet transform to increase matrix sparsity. *Golik* [1998] applied discrete wavelet packet

0048-6604/03/2001RS002475

transform and presented an adaptive algorithm for the selection of the near-best basis transform to sparsify the matrix. *Deng and Ling* [1999a, 1999b] employed adaptive wavelet packet transform and predefined wavelet packet bases to further sparsify the matrix.

[5] In addition, many papers have applied Daubechies wavelets to obtain the matrix sparsification in MoM. Recently, many studies have used different kinds of wavelets to efficiently solve electromagnetic (EM) integral equations. *Pan et al.* [1998, 1999] use the Coifman intervallic wavelets as the basis and testing functions in MoM for fast construction of wavelet-sparisfied matrices. *Huang et al.* [2000] applied Vaidyanathan wavelets based on the quadrature mirror filter to construct the wavelet transform matrix. However, it seems that most of the previous studies did not specify how to choose a proper wavelet for targeting electromagnetic integral equations with oscillatory kernels.

[6] In this paper, we exploit a concept of "visible energy" as a criterion for choosing suitable wavelets in solving electrodynamic scattering problems. Visible energy is defined as the energy of all dilations of a single mother wavelet for an arbitrary translation in the spectral domain over the entire visible region in which the spatial frequency is smaller than the free space spatial frequency (wave number). In the visible region the spectral content of wavelet current becomes the wavelet source that will produce far-field radiation. Since the elements of the wavelet-domain impedance matrix represent the interaction between wavelet sources and receivers, the interaction becomes stronger when more spectral content leaks into the visible region, i.e., greater visible energy. Thus we expect that the quantity of visible energy may reflect the sparsified extent of the impedance matrix. To investigate our concept, numerical simulations are used to solve electromagnetic scattering problems. Different shapes of two-dimensional conducting scatterers such as a circular cylinder, an L-shaped scatterer, and a duct are considered. The combined field integral equation (CFIE) is employed and is solved by the wavelet MoM (WMoM). Note that all the different wavelet basis vectors used here are orthogonal.

2. Constructions of Wavelet Transform of the MoM Impedance Matrix for Electromagnetic Scattering

[7] In electromagnetic scattering problems the current induced on the metallic scatter $f(x)$ is related to the incident field $w(x)$ in the following form:

$$\int_a^b f(x')k(x,x')dx' = w(x)\,, \tag{1}$$

where $k(x)$ is Green's function, acting as the kernel. Here scattering of a transverse magnetic (TM) polarized wave by a two-dimensional conducting object with arbitrary shape is considered. The incident TM wave E_z^{inc} induces a surface current density J_z on the surface of the object, which produces a scattered field E_z^{sca} 2.0*pt*. On the boundary the total field E_z vanishes and yields

$$E_z^{inc}(\mathbf{r}) = -E_z^{\mathrm{sca}}(\mathbf{r}) = -i\omega\mu_0 \oint_c dl' J_z(\mathbf{r}')g_0(\mathbf{r},\mathbf{r}')\,. \tag{2}$$

Here c is the contour of the conducting object, l is length, and g_0 is the two-dimensional Green's function given by

$$g_0(\mathbf{r},\mathbf{r}') = \frac{i}{4}H_0^{(1)}(k_0|\mathbf{r}-\mathbf{r}'|)\,, \tag{3}$$

where $H_0^{(1)}$ is the zero-order Hankel function of first kind and k_0 is the free space wave number. In order to avoid the resonance problem we apply a differential operator $F(r) = 1 + \alpha\hat{n}\cdot\nabla$ to equation (2), which yields the CFIE given by

$$E_z^{\mathrm{inc}}(\mathbf{r}) + \alpha\frac{\partial E_z^{\mathrm{inc}}(\mathbf{r})}{\partial n} = -i\omega\mu_0 \oint_c dl' J_z(\mathbf{r}') \cdot\left[g_0(\mathbf{r},\mathbf{r}') + \alpha\frac{\partial g_0(\mathbf{r},\mathbf{r}')}{\partial n}\right], \tag{4}$$

where the constant α is the CFIE combination parameter and $\partial/\partial n$ is the derivative in the outward normal direction.

[8] Equation (4) is discretized by subdividing contour c into N nonoverlapping pieces of equal length. Then, J_z is described by point matching on a pulse basis, yielding the MoM matrix formulation given by

$$\bar{\mathbf{E}} = \bar{\mathbf{Z}}\cdot\bar{\mathbf{J}}\,, \tag{5}$$

where $\bar{\mathbf{Z}}$ is a full nonsymmetric $N \times N$ matrix and the element Z_{ij} of the matrix $\bar{\mathbf{Z}}$ represents the field radiated by a unit amplitude current pulse j and received at the observation point i; $\bar{\mathbf{J}}$ is a surface current density-related unknown column vector to be solved, and $\bar{\mathbf{E}}$ is the excitation-related column vector. However, because $\bar{\mathbf{Z}}$ is a full matrix, the solution of equation (5) is expensive. For a problem with N unknowns the direct solution of equation (5) has a computational cost of $O(N^3)$. This high solution cost motivates the study of wavelets as a means for sparsifying $\mathbf{Z}$ to obtain an efficient solution.

[9] Let $\mathbf{W}$ be an $N \times N$ wavelet matrix: Carrying out the wavelet matrix transform to equation (5), the wavelet-domain equation is obtained as

$$\tilde{\mathbf{E}} = \tilde{\mathbf{Z}}\cdot\tilde{\mathbf{J}}\,, \tag{6}$$

where $\tilde{\mathbf{Z}} = \mathbf{WZW}^T$, $\tilde{\mathbf{E}} = \mathbf{WE}$, and $\tilde{\mathbf{J}} = (\mathbf{W}^T)^{-1}\mathbf{J}$. Because the vectors of $\mathbf{W}$ form an orthonormal basis for the N-dimensional vector space $\mathbf{R}^N$, $\mathbf{W}$ is an orthogonal matrix satisfying $\mathbf{W}^T = \mathbf{W}^{-1}$, where T stands for the transpose of a matrix. For a given threshold value, equation (6) becomes a sparse matrix which can be efficiently solved by a sparse solver.

3. Visible Energy of Wavelets

[10] Recently, *Wagner and Chew* [1995] analyzed the effectiveness of the wavelet method in terms of the radiation/receiving characteristics of the wavelet basis function. They also demonstrated that in the visible region, where the spatial frequency is smaller than the spatial frequency in free space ($k \leq k_0$), the wavelet currents radiate their spectral content, which induces interaction between wavelet sources and receivers. If this interaction is strong, the number of nonzero elements of the transformed matrix increases. In this section we will extend this finding to exploit a novel concept of "visible energy," which is used as a criterion to select proper wavelets for EM scattering problems. Here the visible energy is defined as the energy of all dilations of a single mother wavelet for an arbitrary translation in the spectral domain over the visible region. Consider a mother wavelet $\Psi(x)$ defined by *Pan* [1996]. The equation of the visible energy is given by

$$E_v = \sum_{l \in \mathbf{Z}} \sum_{k \leq k_0} \|\hat{\Psi}_{l,m}(k)\|^2, \tag{7}$$

where $\hat{\Psi}_{l,m}(k)$ is the Fourier transform of $\Psi_{l,m}(x)$. Note that $\{\Psi_{l,m}(x) = 2^{l/2}\Psi(2^l x - m) \mid l, m \in \mathbf{Z}\}$ forms a Riesz basis for $L^2(\mathbf{R})$, where $\mathbf{R}$ is the set of all real numbers. Let us consider an $N \times N$ ($2^n \times 2^n$) matrix $\mathbf{W}$ formed by wavelets; the visible energy may then be computed by the following equation:

$$E_v = \sum_{i=1}^{\log_2 N - 1} \sum_{j=1}^{\left[\frac{N}{M}\right]} \|[\varpi_{ij}]\|^2. \tag{8}$$

The matrix $[\varpi_{ij}]$ of equation (8) is of dimension $(\log_2 N - 1) \times N$, and the ith row of the matrix is defined to be the Fourier transform of row a_i of the wavelet matrix $\mathbf{W}$, where a_i is given by

$$a_i = \begin{cases} \dfrac{\mathrm{N}}{2^{\mathrm{i}+1}} & \mathrm{i}=1 \\ \dfrac{\mathrm{N}}{2^{\mathrm{i}+1}} + \displaystyle\sum_{\mathrm{p}=1}^{\mathrm{i}-1} \dfrac{\mathrm{N}}{2^{\mathrm{p}}}, & \mathrm{i}=2 \ldots \log_2 N - 1 \end{cases} \tag{9}$$

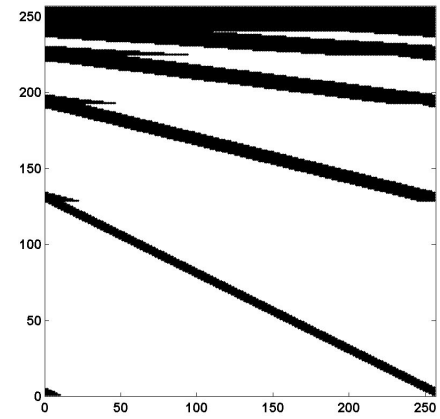

Figure 1. Magnitude of the basis vector matrix $\mathbf{W}$ for the Daubechies wavelets with number of discretization points $N = 256$ and vanishing moments $p = 5$. Each row is one basis vector.

where p is vanishing moments. The row index a_i is designed to sample one wavelet basis for an arbitrary translation of each resolution scale of the wavelet matrix $\mathbf{W}$. Here the centered translation row index of each resolution scale is chosen for the computation of visible energy. A discretization density of M points per wavelength for the scaling of the spatial frequency axis is assumed. In order to quantify the visible energy from these sample basis vectors at rows a_i in the visible region, where the spatial frequency is smaller than the spatial frequency in free space ($k/k_0 \leq 1$), the column j of the matrix $[\varpi_{ij}]$ within limits $1 \leq j \leq [N/M]$ is just required.

[11] Figure 1illustrates a gray scale image (magnitude) of the basis vector matrix $\mathbf{W}$ for Daubechies wavelets with number of discretization points $N = 256$ and vanishing moments $p = 5$. It is known that each row of the wavelet matrix stands for a wavelet basis. The different bands in the image correspond to different resolution scales in the basis. Sample basis vectors of $\mathbf{W}$ at rows (a_i) 64, 160, 208, 232, 244, 250, and 253 are shown in Figure 2. The basis vectors form a complete orthonormal basis for N-dimensional wavelet vector space $\mathbf{R}^N$. These basis vectors are true wavelets as can be seen in Figure 2; they are all translations and dilations of a single mother wavelet. Translations of the finest resolution wavelet compose one half of the basis set; translations of the next finest resolution wavelet make up one quarter of the set and so on down the hierarchy. Magnitude spectra of these basis vectors with a discretization density of 10 points per unit wavelength are shown in Figure 3. It is apparent that the broader spatial support of wavelets has more spectral content extending into the visible region.

[12] Table 1 lists the visible energy of some well-known wavelets such as Daubechies, Coifman, Beylkin,

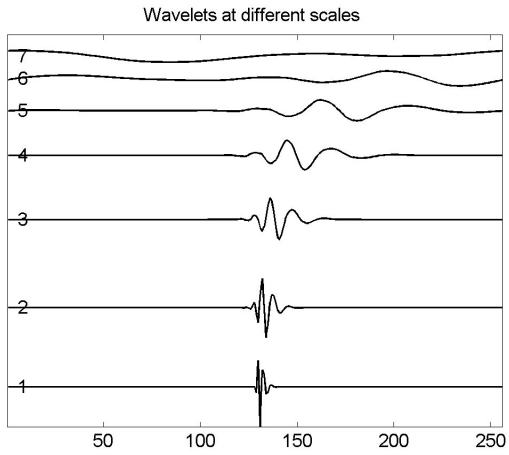

Figure 2. Sample basis vectors for the Daubechies wavelets with discretization points $N = 256$ and vanishing moments $p = 5$.

and Vaidyanathan wavelets, which are also referred to as orthogonal filters, assuming a discretization density of 10 points per unit wavelength. From Table 1 it is also found that the visible energy is decreased when the filter length l_c of the wavelet is increased. The reason for this is that the larger filter length produces smoother, broader basis functions whose magnitude spectra of wavelet have sharper spectral cutoffs, so less spectra leaks into the visible region. Additionally, the visible energy is increased as the matrix size is increased because a larger number of different scales of wavelets leak their spectra into the visible region.

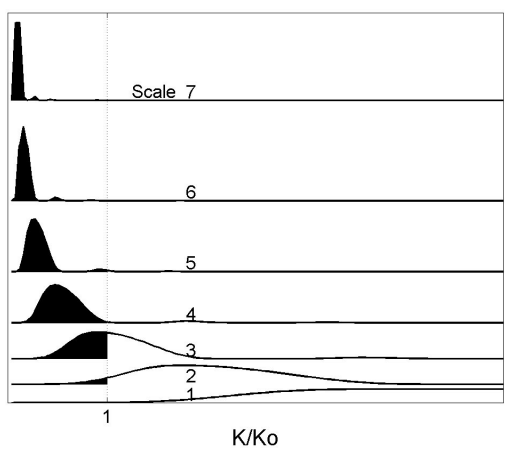

Figure 3. Magnitude spectra of sample basis vectors with a discretization density of 10 points per wavelength given in Figure 1.

4. Numerical Results and Discussions

[13] In this section, we investigate the relation between the matrix sparsity and visible energy through some numerical examples. In the examples, three two-dimensional scatterers, including a circular cylinder, an L-shape scatterer, and a duct, are chosen. The geometry of each problem is shown in Figure 4. Here the excited TM (E_z) polarized planar wave is incident from 0° into the circular cylinder and 45° into the L-shaped or duct scatterer. To avoid internal resonance, CFIE is employed to generate the moment matrices by using a discretization size of 0.1 λ. Both the MoM and WMoM are applied to solve the surface currents induced on the conducting scatterer with relative residual error $\|\mathbf{E}' - \mathbf{Z}'\mathbf{J}'\|/\|\mathbf{E}'\| = (1 \pm 0.01)$ %. Note that in WMoM all the different wavelet basis vectors chosen here are orthonormal and that their discrete wavelet transform matrices are orthogonal. Figures 5, 6, and 7 show the computed magnitudes of the induced current densities for the circular cylinder, the L-shaped scatterer, and the duct, respectively. It is found that the solution accuracy of MoM and WMoM is almost the same when the residual error is fixed at 1%.

[14] For the circular cylinder case the nonzero-element percentages of the transformed matrix versus visible energy for different kinds of orthogonal wavelets are presented in Figure 8. Cases of different filter length and matrix size are considered. It is found that for fixed matrix size the greater the visible energy of the wavelet, the less matrix sparsity is seen. This is because greater visible energy leads to more spectral content radiation, which induces strong interaction between wavelet sources and receivers. This yields a larger number of nonzero elements to the transformed matrix.

[15] The larger filter length of the wavelets is, the lower the visible energy is and the higher the compression rate of the matrix is. However, larger filter lengths would result in more basis vectors and need more computation time to solve the sparsified matrix. Therefore, when choosing a particular wavelet, we thus face a trade-off between the visible energy and filter length. Figure 9 illustrates the visible energy and matrix sparsity as a function of filter lengths of Daubechies wavelets. It is apparent that both curves have a similar trend. The percentage of the nonzero elements of the wavelet matrix and visible energy both have larger decreasing slope in the range of $l_c < 24$ than in the range of $l_c > 24$. This means that it is not worth increasing the filter length in the range of $l_c > 24$ since the sparsification only increases slightly and vice versa. The results were confirmed by *Sarkar et al.* [1998]. For a large object scattering problem, time savings due to the increase of matrix sparsification

Table 1. Visible Energy E_v of Some Well-Known Orthogonal Wavelet Filters With Various Filter Lengths l_c and Matrix Sizes N[a]

	Matrix Size				
Wavelet Filter	128	256	512	1024	2048
Daubechies 6	4.9988+03	2.8192+04	1.3735+04	6.1447+05	2.6487+06
Daubechies 12	4.0111+03	2.1909+04	1.0485+04	4.6401+05	1.9856+06
Daubechies 18	3.6266+03	1.9565+04	9.3127+04	4.1080+05	1.7542+06
Daubechies 24	3.4270+03	1.8354+04	8.7074+04	3.8332+05	1.6347+06
Daubechies 30	3.3042+03	1.7607+04	8.3320+04	3.6622+05	1.5602+06
Coifman 6	5.2366+03	2.9795+04	1.4615+04	6.5700+05	2.8419+06
Coifman 12	4.4675+03	2.4757+04	1.1935+04	5.3034+05	2.2756+06
Coifman 18	3.9483+03	2.1523+04	1.0291+04	4.5517+05	1.9470+06
Coifman 24	3.6704+03	1.9828+04	9.4435+04	4.1670+05	1.7798+06
Coifman 30	3.4996+03	1.8793+04	8.8262+04	3.9323+05	1.6778+06
Vaidyanathan 16	3.4975+03	1.8789+04	8.9279+04	3.9343+05	1.6789+06
Vaidyanathan 24	3.1553+03	1.6700+04	7.8747+04	3.4537+05	1.4693+06
Beylkin 18	3.2458+03	1.7237+04	8.1374+04	3.5711+05	1.5189+06

[a]A discretization density of 10 points per wavelength is assumed. Visible energy E_v is in e.

effectively compensates the computational time increase because of increasing filter length.

[16] Similar results are presented in Figures 10 and 11 for an L-shaped scatterer and a duct, respectively. However, when the matrix size is small ($N \leq 512$), the smaller visible energy may not lead to greater matrix sparsity, especially for wavelets with a larger filter length, such as Daubechies 24, Daubechies 30, Coifman 24, Coifman 30, and Vaidyanathan 24. This is because the large-filter-length wavelets will result in more wavelet basis vectors than those with a small filter length. A small scatterer with several corners may produce extra interactions among wavelet basis vectors compared with the case of using wavelets with larger filter lengths. This could adversely affect the matrix sparsity. However, for larger object scatter problems the geometrical bending effects will be diminished.

[17] Fortunately, our finding is still useful since the direct solution of conventional MoM equations is prohibitively expensive for large-scale scattering problems. Our results suggest that when the matrix size is large (for large scattering objects), using wavelets with smaller visible energy leads to a greater sparsification of the matrix.

5. Summary

[18] In this paper, we show that the use of visible energy can help in choosing proper orthogonal wavelets to solve EM integral problems. It is found that for large scattering object problems or the circular cylinder problems the wavelets with smaller visible energy lead to greater wavelet-domain impedance matrix sparsity. This result may not be true for the cases of small L-shaped or

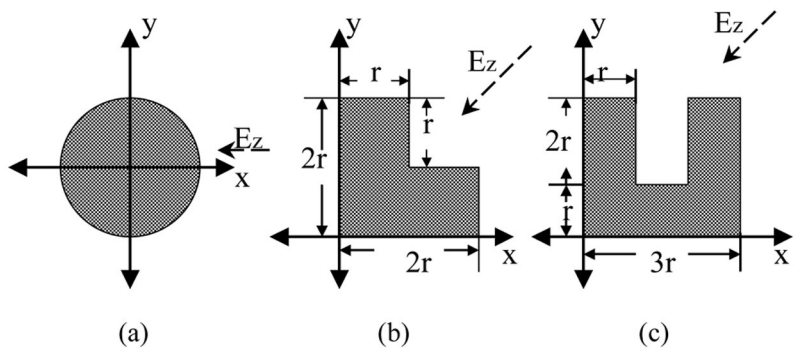

Figure 4. The geometry of the three test scatterers: (a) a circular cylinder, (b) an L-shaped scatterer, and (c) a duct.

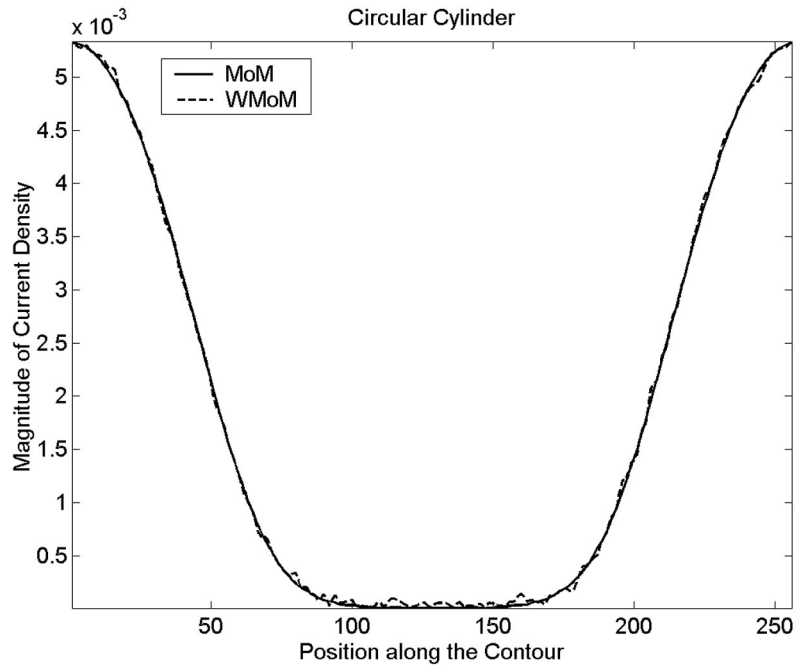

Figure 5. Magnitude of the surface current density for a circular cylinder with contour length 25.6 λ and discretized with $N = 256$ (Daubechies 18).

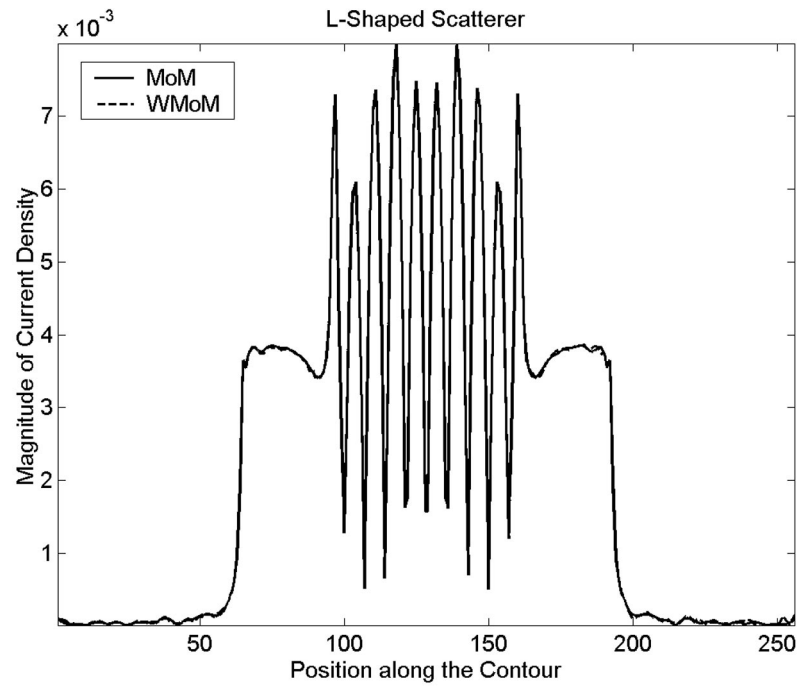

Figure 6. Magnitude of the surface current density for an L-shaped scatterer with contour length 25.6 λ and discretized with $N = 256$ (Daubechies 18).

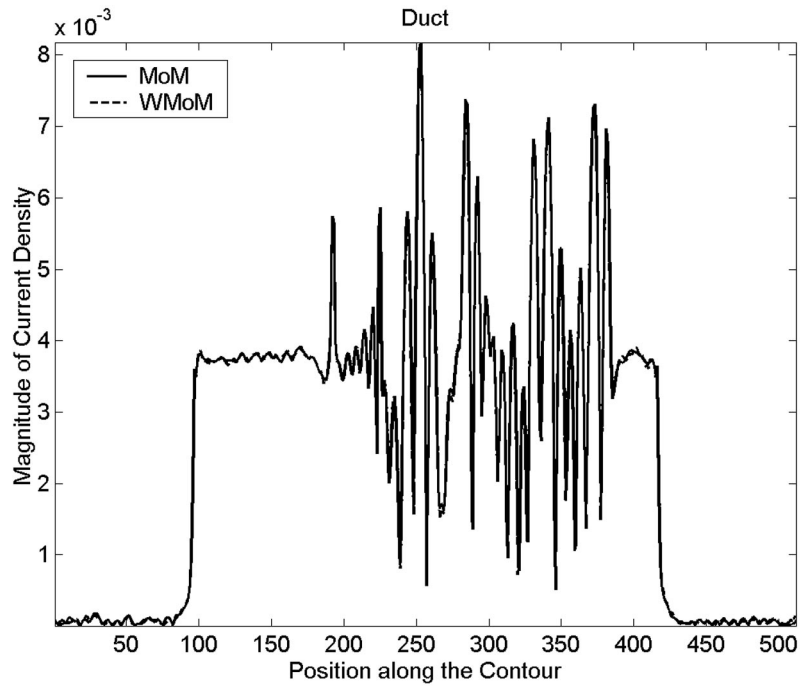

Figure 7. Magnitude of the surface current density for a duct with contour length 51.2 λ and discretized with $N = 512$ (Daubechies 18).

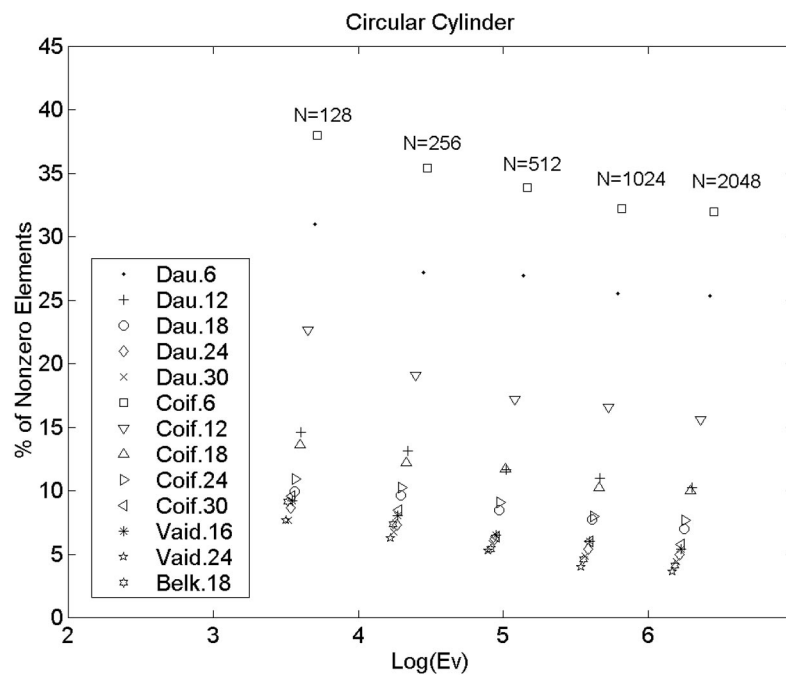

Figure 8. Matrix sparsity as a function of visible energy for a circular cylinder with different kinds of wavelets and matrix sizes N.

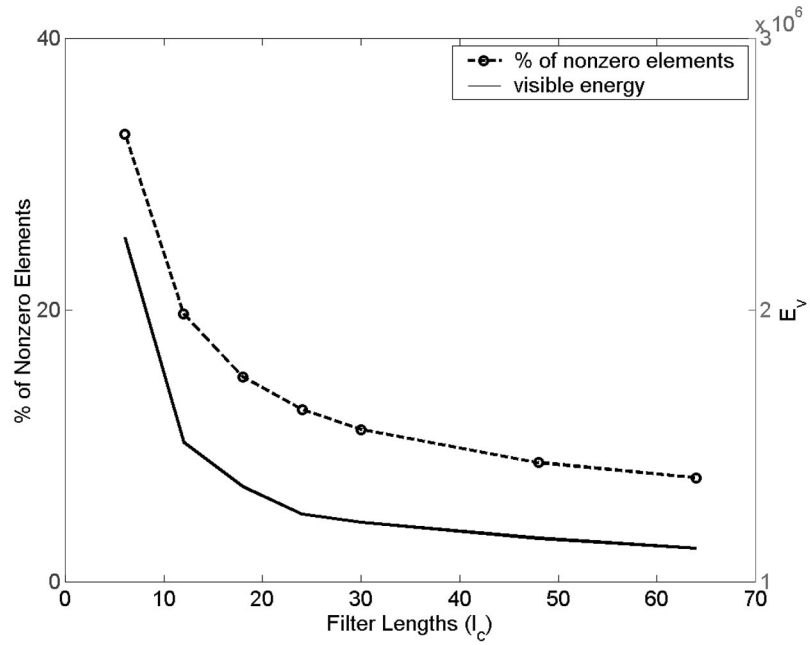

Figure 9. Matrix sparsity and visible energy (E_v) as a function of filter length with matrix size N = 2048. The Daubechies wavelets were used.

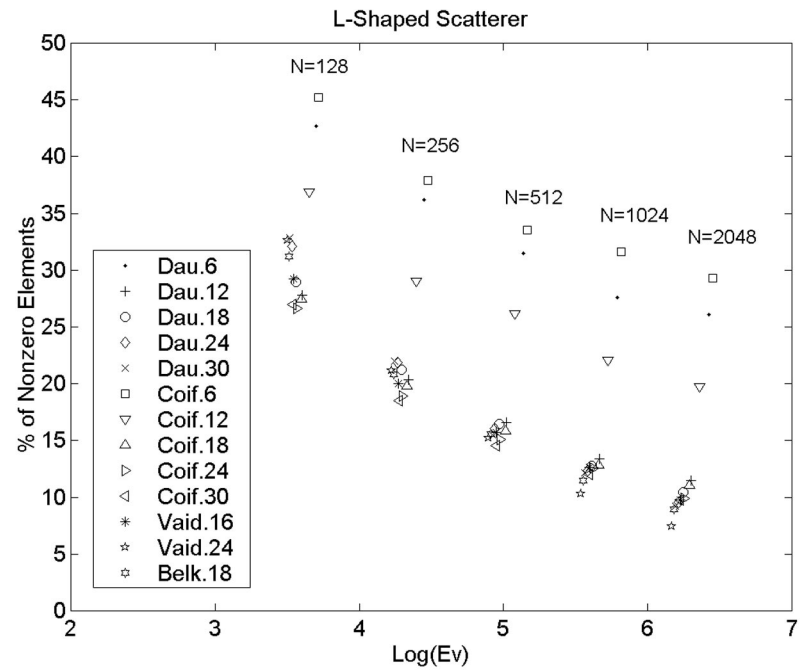

Figure 10. Matrix sparsity as a function of visible energy for an L-shaped scatterer with different kinds of wavelets and matrix sizes N.

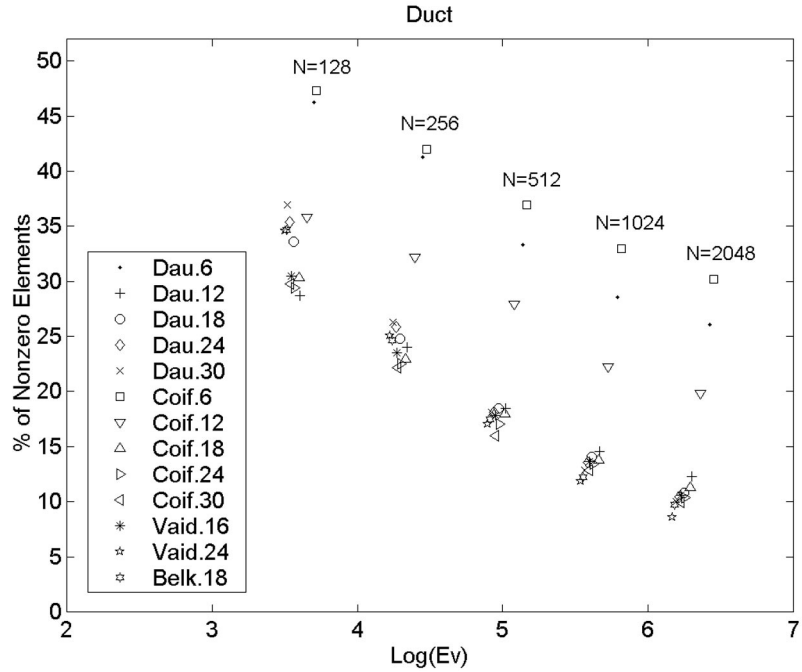

Figure 11. Matrix sparsity as a function of visible energy for a duct with different kinds of wavelets and matrix sizes *N*.

duct scatterers. However, our finding remains useful since the direct solution of conventional MoM equations is prohibitively expensive for large-scale scattering problems. The analysis in this paper only considers the orthogonal wavelets. In the near future the same principle will be validated for nonorthonormal wavelets.

[19] **Acknowledgments.** This work was sponsored jointly by the Ministry of Education and the National Science Council, ROC, under contract 89-E-FA06-2-4/X89018.

References

Bernardi, P., I. R. Cicchetti, and A. Faraone, A full-wave characterization of an interconnecting line printed on a dielectric slab backed by a gridded ground plane, *IEEE Trans. Electromagn. Compat.*, *38*(3), 237–243, 1996.

Beylkin, G., R. Coifman, and V. Rokhlin, Fast wavelet transforms and numerical algorithms I, *Commun. Pure Appl. Math.*, *44*, 141–183, 1991.

Christopoulos, C., and J. L. Herring, The application of transmission-line modeling (TLM) to electromagnetic compatibility problems, *IEEE Trans. Electromagn. Compat.*, *35*(2), 185–191, 1993.

D'amore, M., and M. S. Sarto, Simulation models of a dissipative transmission line above a lossy ground for a wide-frequency range, II, Multiconductor configuration, *IEEE Trans. Electromagn. Compat.*, *38*(2), 139–149, 1996.

Deng, H., and H. Ling, Fast solution of electromagnetic integral equations using adaptive wavelet packet transform, *IEEE Trans. Antennas Propag.*, *47*(4), 674–682, 1999a.

Deng, H., and H. Ling, On a class of predefined wavelet packet bases for efficient representation of electromagnetic integral equations, *IEEE Trans. Antennas Propag.*, *47*(12), 1772–1779, 1999b.

Dixon, D. S., M. Obara, and N. Schade, Finite-element analysis as an EMC prediction tool, *IEEE Trans. Electromagn. Compat.*, *35*(2), 241–248, 1993.

Golik, W. L., Wavelet packets for fast solution of electromagnetic integral equations, *IEEE Trans. Antennas Propag.*, *46*(5), 618–624, 1998.

Harrington, R. F., *Field Computation by Moment Methods*, Macmillan, Old Tappan, N. J., 1968.

Holland, R., V. P. Cable, and L. C. Wilson, Finite-volume time-domain (FVTD) techniques for EM scattering, *IEEE Trans. Electromagn. Compat.*, *33*(4), 281–294, 1991.

Huang, J. M., J. L. Leou, S. K. Jeng, and J. H. Tarng, Impedance matrix compression using effective quadrature filter, *Proc. IEE Microwaves Antennas Propag.*, *147*(4), 255–260, 2000.

Kim, H., H. Ling, and C. Lee, A fast moment method algorithm using spectral domain wavelet concepts, *Radio Sci.*, *31*, 1253–1261, 1996.

Miller, E. K., and J. A. Landt, Direct time-domain technique for transient radiation and scattering from wires,

Proc. IEEE, *18*, 1396–1423, 1980.

Pan, G., Orthogonal wavelets with applications in electromagnetics, *IEEE Trans. Magn.*, *32*(3), 975–983, 1996.

Pan, G., M. Toupikov, J. Du, and B. K. Gilbert, Use of Coifman intervallic wavelets in 2-D and 3-D scattering problems, *Proc. IEE Microwaves Antennas Propag.*, *145*(6), 471–480, 1998.

Pan, G., M. Toupikov, and B. K. Gilbert, On the use of Coifman intervallic wavelets in the method of moments for fast construction of wavelet sparsified matrices, *IEEE Trans. Antennas Propag.*, *47*(7), 1189–1200, 1999.

Sacks, Z. S., and J.-F. Lee, A finite-element time-domain method using prism elements for microwave cavities, *IEEE Trans. Electromagn. Compat.*, *37*(4), 519–527, 1995.

Sarkar, T. K., C. Su, R. Adve, M. Salazar-Palma, L. Garcia-Castillo, and R. R. Boix, Tutorial on wavelets from an electrical engineering perspective, part 1: Discrete wavelet techniques, *IEEE Antennas Propag. Mag.*, *40*(5), 49–70, 1998.

Taflove, A., and K. R. Umashankar, Review of FDTD numerical modeling of electromagnetic wave scattering and radar cross section, *Proc. IEEE*, *77*(5), 682–699, 1989.

Tirkas, P. A., C. A. Balanis, M. P. Purchine, and G. C. Barber, Finite-difference time-domain method for electromagnetics, radiation, interference, and interaction with complex structure, *IEEE Trans. Electromagn. Compat.*, *35*(2), 192–203, 1993.

Wagner, R. L., and W. C. Chew, A study of wavelets for the solution of electromagnetic integral equations, *IEEE Trans. Antennas Propag.*, *43*(8), 802–810, 1995.

C.-M. Chen, J.-M. Huang, and J.-H. Tarng, Department of Communication Engineering and Microelectronics and Information Systems Research Center, National Chiao Tung University, Hsin-Chu, Taiwan. (jimmy@cht.com.tw; j4t@cc.nctu.edu.tw)